



# EEG resting state analysis of cortical sources in patients with benign epilepsy with centrotemporal spikes



Azeez Adebimpe<sup>a</sup>, Ardalan Aarabi<sup>a,\*</sup>, Emilie Bourel-Ponchel<sup>b</sup>, Mahdi Mahmoudzadeh<sup>a,b</sup>, Fabrice Wallois<sup>a,b</sup>

<sup>a</sup>INSERM U 1105, CURS, CHU sud, Salouël, Av. Laennec, 80054 Amiens Cedex, France

<sup>b</sup>INSERM U 1105, EFSN Pédiatriques, CHU sud, Salouël, Av. Laennec, 80054 Amiens Cedex, France

## ARTICLE INFO

### Article history:

Received 18 February 2015

Received in revised form 19 August 2015

Accepted 20 August 2015

Available online 3 September 2015

### Keywords:

Benign epilepsy

Centrotemporal spikes

Spectral power

Source analysis

EEG

## ABSTRACT

Benign epilepsy with centrotemporal spikes (BECTS) is the most common idiopathic childhood epilepsy, which is often associated with developmental disorders in children. In the present study, we analyzed resting state EEG spectral changes in the sensor and source spaces in eight BECTS patients compared with nine age-matched controls. Using high-resolution scalp EEG data, we assessed statistical differences in spatial distributions of EEG power spectra and cortical sources of resting state EEG rhythms in five frequency bands:  $\delta$  (0.5–3.5 Hz),  $\theta$  (4–8 Hz),  $\alpha$  (8.5–13 Hz),  $\beta_1$  (13.5–20 Hz) and  $\beta_2$  (20.5–30 Hz) under the eyes-closed resting state condition. To further investigate the impact of centrotemporal spikes on EEG spectra, we split the EEG data of the patient group into EEG portions with and without spikes. Source localization demonstrated the homogeneity of our population of BECTS patients with a common epileptic zone over the right centrotemporal region. Significant differences in terms of both spectral power and cortical source densities were observed between controls and patients. Patients were characterized by significantly increased relative power in  $\theta$ ,  $\alpha$ ,  $\beta_1$  and  $\beta_2$  bands in the right centrotemporal areas over the spike zone and in the right temporo-parieto-occipital junction. Furthermore, the relative power in all bands significantly decreased in the bilateral frontal and parieto-occipital areas of patients regardless of the presence or absence of spikes in EEG segments. However, the spectral differences between patients and controls were more pronounced in the presence of spikes. This observation emphasized the impact of benign epilepsy on cortical source power, especially in the right centrotemporal regions. Spectral changes in bilateral frontal and parieto-occipital areas may also suggest alterations in the default mode network in BECTS patients.

© 2015 The Authors. Published by Elsevier Inc. This is an open access article under the CC BY-NC-ND license (<http://creativecommons.org/licenses/by-nc-nd/4.0/>).

## 1. Introduction

Benign epilepsy, also known as Rolandic epilepsy, is the most common idiopathic childhood epilepsy with a prevalence of approximately 15% in children aged 1–15 years (Panayiotopoulos et al., 2008). Rolandic epilepsy is characterized by seizures that typically originate in the centrotemporal area with often the same sensorimotor symptoms and autonomic manifestations in the face, mouth and throat (Loiseau, 2001; Loiseau and Beaussart, 1973). The majority of Rolandic seizures occur during non-REM sleep, at sleep onset or rest (Camfield et al., 2014; Panayiotopoulos et al., 2008; Shields and Snead, 2009). As the hallmark of benign childhood epilepsy, seizures are mostly associated with centrotemporal spikes (CTS) often followed by slow waves, which are typically activated by drowsiness and slow (non-REM) sleep (Blom and Brorson, 1966; Clemens and Majoros, 1987; Smith and Kellaway, 1964). Dipole source localization in patients with BECTS has demonstrated that CTS can be reliably modeled by single tangential dipole sources oriented from central to frontal lobes and localized in the

high and low central regions (suprasylvian) (Gregory and Wong, 1992; Jung et al., 2003; Legarda et al., 1994; Panayiotopoulos, 1999b; Tsai and Hung, 1998). Despite the focality of CTS and rolandic seizures in patients with benign epilepsy, there is growing evidence from neuroimaging studies reporting memory, language, attention, auditory and cognitive impairments in BECTS patients that BECTS may functionally and structurally affect a larger portion of the brain at rest (Bocquillon et al., 2009; Cataldi et al., 2013; Lopes et al., 2014; Northcott et al., 2007; Verrotti et al., 2014).

The present study attempted to investigate changes in the spectral power and spatial distribution of cortical sources of eyes-closed resting state EEG rhythms in patients with BECTS compared to healthy subjects under two conditions, in the presence and absence of CTS.

## 2. Methods

### 2.1. Subjects

Twenty-one children ( $9.84 \pm 1.75$  years) with BECTS and 12 healthy subjects ( $9.27 \pm 1.70$  years) used as controls were preselected for resting state analysis. The study was conducted at Amiens University

\* Corresponding author.

E-mail address: [ardalan.aarabi@u-picardie.fr](mailto:ardalan.aarabi@u-picardie.fr) (A. Aarabi).

**Table 1**  
Characteristics of the control and patient groups.

Control group			Patient group					
Subject	Age (years)	EEG duration (min)	Patient	Age (years)	EEG duration (min)	Neuropsychological assessment	Description of ictal EEG	Medication
1	6.73	16.21	1	12.63	50.84	Normal	Partial seizure	Sodium valproate
2	11.28	19.59	2	12.64	17.85	Normal	Partial seizure	Sodium valproate
3	10.48	19.75	3	9.25	44.08	Attention deficit	Generalized tonic-clonic seizure	Oxcarbazepine
4	10.66	17.44	4	6.03	43.52	–	Brachiofacial nocturnal seizure	Oxcarbazepine
5	7.39	13.54	5	10.47	50.06	Attention deficit	Partial seizure	Sodium valproate
6	7.31	20.30	6	7.16	14.26	–	Brachiofacial nocturnal seizure	Sodium valproate
7	11.92	30.02	7	8.51	30.36	Attention deficit	Nocturnal seizure	–
8	8.44	75.00	8	13.16	20.02	Normal	Generalized tonic-clonic seizure	Sodium valproate
9	9.36	28.00	9	9.67	15.63	Language deficit	Generalized tonic-clonic seizure	Lamotrigine
10	9.48	45.09	10	7.79	23.12	Normal	Generalized tonic-clonic seizure	Micropakine
11	10.32	18.97	11	8.91	16.78	Normal	Generalized tonic-clonic seizure	Trileptal
12	7.98							
Mean $\pm$ SD	9.27 $\pm$ 1.70			9.65 $\pm$ 2.36				

Hospital (France) and was approved by the hospital's ethics committee (CPP Nord-Ouest No: 2011-A00782-39). Written informed consent was obtained from each subject's caregivers. Healthy subjects had no history of neurological disorders. Patients showed no structural brain abnormalities on MRI.

## 2.2. Data acquisition and preprocessing

An EEG lasting at least 14 min was recorded in each individual at a sampling rate of 256 Hz with a high-resolution EEG recording system (ANT, Netherlands) using 64 electrodes placed on the scalp according to the international 10–10 system. Forehead ground and linked-ear reference electrodes were used for data collection. During the recordings, the subjects were asked to rest comfortably in a supine position in a quiet dark room and were instructed to stay fully relaxed and motionless. We made sure that they were fully awake during data collection. Since the reference electrode could be contaminated by ocular artifacts, EEG data were offline re-referenced to common average reference and filtered between 0.5 to 30 Hz to remove possible high frequency noise. Two experienced neurophysiologists visually inspected the EEG data to identify centrotemporal spikes.

To define a homogeneous group of patients, we first identified the location of interictal sources for each patient using the spatiotemporal dipole modeling method (Advanced Source Analysis Software, Enschede, The Netherlands) (Scherg and Von Cramon, 1985). To define a homogeneous sample of patients for both single subject and group analyses, eleven of the twenty-one patients (9.65  $\pm$  2.36 years) with right centrotemporal spikes were selected to form the epileptic group. Table 1 lists the characteristics of patients and controls and a summary of their EEG records. Three of the eight patients were diagnosed with attention deficit hyperactivity disorder. Fig. 1 shows the EEG dipole source localization results projected onto the MRI template and sample EEG of one of the patients.

To identify EEG portions with ocular and movement artifacts, the EEG recordings were first normalized by the Z-score transformation and then processed semi-automatically using a threshold method as it was implemented in Fieldtrip software<sup>1</sup> (Oostenveld et al., 2011). For each channel, EEG portions that exceeded a predefined threshold were marked and visually inspected by the experts. The threshold was set to the mean plus one standard deviation of the z-score amplitude distribution for each channel. The artifact-free eyes-closed portions of the EEG recordings were then segmented into non-overlapping 2-s epochs. In this study, all statistical comparisons were performed

between controls and patients under the eyes-closed (EC) condition. To study the effect of interictal spikes on the dynamics of EEG and cortical sources during the resting state, patients were compared with controls under two conditions, EC<sub>NS</sub> (eyes-closed without spike) and EC<sub>WS</sub> (eyes-closed with spike). Five segments were randomly selected for each subject and condition for further analysis. The EC<sub>WS</sub> EEG segments contained an average of 7 spikes as a requirement to ensure homogeneity across the patients.

## 2.3. EEG spectral analysis

The absolute power spectral density for each channel and EEG segment was computed by using the multi-taper method with Slepian sequences (Jarvis and Mitra, 2001; Mitra and Pesaran, 1999) with a frequency resolution of 0.5 Hz. Multi-taper frequency method is similar to the classical Fourier transform but it is frequency specific with very good anti-frequency leakage properties (van Vugt et al., 2007). Power spectral analysis was performed using the Fieldtrip toolbox (<http://www.ru.nl/donders/fieldtrip>) (Oostenveld et al., 2011). To investigate homogeneity across patients and controls, we computed individual alpha frequency (IAF) as described by Klimesch (1999) and Klimesch et al. (1993). IAF was calculated as the sum of the product of the spectral power estimates and the frequency divided by the total sum of spectral power estimates within  $\alpha$  band. This method has shown to be more robust and adequate particularly if there are multiple peaks in the  $\alpha$  range (Klimesch, 1999).

For statistical analysis, the whole frequency range (0.5–30 Hz) was reduced into five frequency bands:  $\delta$  (0.5–3.5 Hz),  $\theta$  (4.0–8.0 Hz),  $\alpha$  (8.5–13.0 Hz),  $\beta_1$  (13.5–20.0 Hz) and  $\beta_2$  (20.5–30 Hz), corresponding to the most common frequency bands in all epileptic patients and healthy subjects.

For each channel and each subject, the power spectrum was then averaged over all five segments. The relative power spectrum was then obtained by normalizing the power spectral density of each channel to its total power.

To reduce the spatial dimensionality of the data, we first grouped the 63 channels into 13 brain regions as shown in Fig. 2. For each region and frequency band, we reported absolute and relative spectral power. We then compared regional relative spectral powers within each frequency band between groups by computing across-subject grand average Scalp Topographic Patterns (STPs) of relative EEG spectral power (STP,  $\pm$  standard deviation) for each frequency band and group. The statistical analysis was performed in each region including four electrodes on average. The group comparison was performed by the standard nonparametric paired two-way ANOVA with 5000 permutations and  $p < 0.01$  (Maris and Oostenveld, 2007).

<sup>1</sup> [http://www.fieldtriptoolbox.org/tutorial/visual\\_artifact\\_rejection](http://www.fieldtriptoolbox.org/tutorial/visual_artifact_rejection).

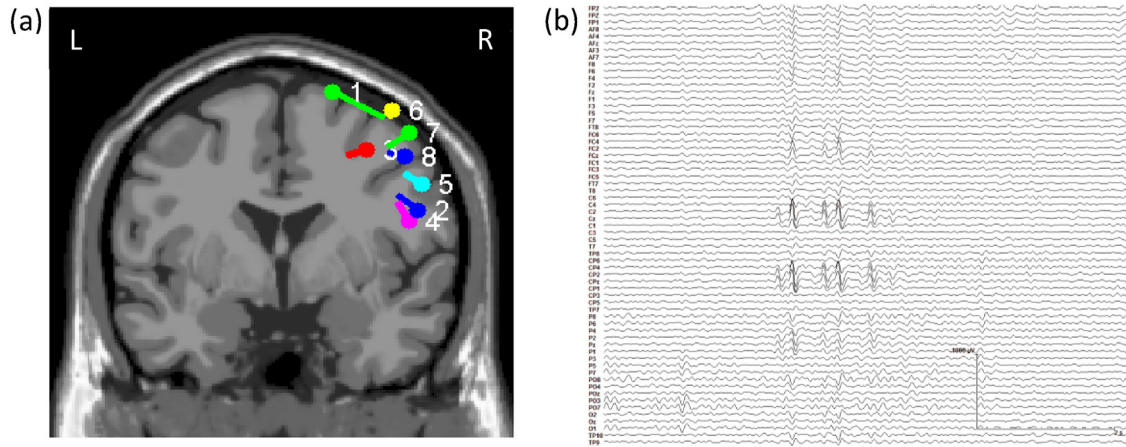


Fig. 1. (a) Dipole locations of the averaged spikes for patients, and (b) a sample EEG recording from patient 1.

2.4. EEG source distribution analysis using eLORETA

EEG cortical source analysis was performed by the functional brain imaging method known as eLORETA (exact Low-Resolution Electromagnetic Tomography), which models 3D distributions of EEG cortical sources (Grech et al., 2008; Pascual-Marqui, 2002, 1999) in the frequency domain. This method does not require a priori knowledge of dipole positions and has been successfully used in recent studies on resting state EEG analysis (Babiloni et al., 2010; Li, 2010). eLORETA is a discrete, linear, weighted minimum norm inverse solution and provides better accurate localization of highly correlated point sources with low signal to noise ratio data (Pascual-Marqui, 2007; Pascual-Marqui et al., 2011). We first used eLORETA to localize interictal spike sources for each patient to investigate the spatial extent of spike sources.

3D source localization in the frequency domain was then performed by computing the cross-spectra of EEG segments for each subject. The eLORETA algorithm was used to compute the current density (Intensity of the current/area, measured in A/m<sup>2</sup>) for each voxel within different frequency bands. The eLORETA solution space was restricted to the cortical gray matter of a realistic head model (MNI152) coregistered to the Talairach brain atlas and digitized at the Montreal Neurologic Institute (MNI) brain imaging center (Mazziotta et al., 2001). The brain compartment included 6239 voxels (5 mm spatial resolution). Before any

statistical analysis, the eLORETA solutions were normalized for each voxel at each frequency band as implemented in the eLORETA software (Pascual-Marqui, 2002). The normalization was done by normalizing the eLORETA current density at each voxel to the eLORETA current density averaged across all frequencies (0.5–30 Hz) (Babiloni et al., 2010).

2.5. Statistical analysis of the eLORETA solutions

Statistical comparisons of cortical sources between the two groups were performed on the eLORETA current density of the voxels in all five frequency bands using the statistical nonparametric mapping approach (SnPM) via randomizations (Nichols and Holmes, 2002). The randomization determined the critical threshold values for the observed t-values with correction ( $p < 0.05$ ) for multiple comparisons across all voxels and all frequency bands. A total of 5000 permutations were used to determine the significance level for each test. The log of F-ratios were then color-coded and projected onto the MNI152 MRI and the cortical layer of the realistic head model. The color-coded Topographic Significance Maps (TSMs) represented statistical differences in estimated cortical sources between the groups.

3. Results

For illustrative purposes, we only present STP (sensor space) and TSM (source space) with statistically distinct spatial patterns. The remaining results can be found in Supplementary Materials. The absolute power for all the conditions is shown in Table 2.

3.1. Scalp topographic patterns (STP)

Fig. 3 shows the STPs for controls and patients in the  $\delta$ ,  $\theta$  and  $\alpha$  bands.

Compared to controls, the patient group presented significantly higher relative EEG power values in the  $\theta$  band (Fig. 3, left STP map) in right centrotemporal and bilateral frontal and parieto-occipital areas under EC<sub>NS</sub> and EC<sub>WS</sub> conditions. The  $\theta$  power increases in all cortical regions were more pronounced when spikes were included in the EEG segments analyzed (EC<sub>WS</sub> condition). In contrast, the relative  $\alpha$ ,  $\beta_1$  and  $\beta_2$  powers tended to decrease in homologous areas especially under the EC<sub>NS</sub> condition (Figs. 3 and S1). Furthermore, relative  $\delta$  power significantly decreased in right centrotemporal and bilateral frontal areas, but only in the presence of CTS. The results obtained in the sensor space are summarized in Table 2. Table 3 lists the mean and standard deviation of absolute power values for each region, frequency band and condition. As shown, patients displayed increased absolute  $\theta$  power and decreased absolute  $\alpha$  power at the parietal and

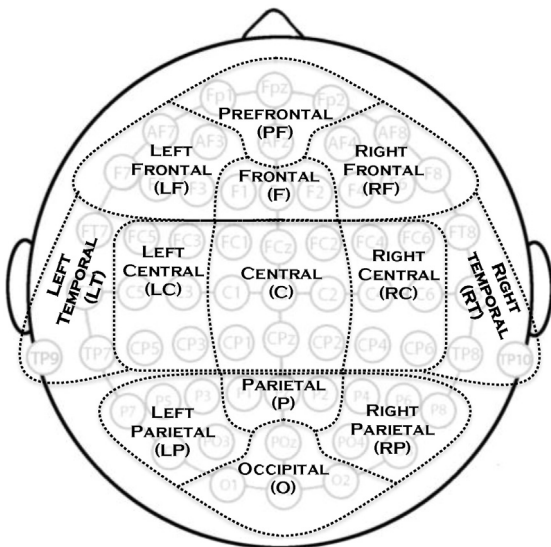


Fig. 2. Thirteen brain regions defined for statistical comparisons.

**Table 2**

Observed patterns of changes in relative EEG spectral power in patients compared to controls in the five frequency bands.

Frequency band	EC <sub>NS</sub> condition (eyes-closed without spike)	EC <sub>WS</sub> condition (eyes-closed with spike)
	Brain regions exhibiting significant changes in scalp EEG relative power	Brain regions exhibiting significant changes in scalp EEG relative power
$\delta$ (0–3.5Hz)	-	LF, RF ↓ C, RC, RT ↓
$\theta$ (4–8Hz)	C, RC, RT ↑ LP, P, RP ↑	All cortical regions ↑
$\alpha$ (8.5–13Hz)	PF, LF, RF ↓ LT, RC ↑ LP, P, RP, O ↓	LP, P, RP, O ↓
$\beta_1$ (13.5–20Hz)	PF ↓ C, RC ↓ LP, P, RP, O ↓	C, RP ↓
$\beta_2$ (20.5–30Hz)	PF ↓ RC, C, LC ↓ LP, P, RP, O ↓	PF, LF, F ↓ C, RC ↓ LP, P, RP, O ↓

The significant increase (↑) or decrease (↓) in EEG relative power was identified by statistical comparisons ( $p < 0.01$ ) between controls and patients. See Fig. 1 for the abbreviations used for brain regions.

occipital regions especially under the EC<sub>WS</sub> conditions in comparison to EC<sub>CT</sub>.

The group IAF values are shown in Fig. 4. The IAF values of EC<sub>CT</sub> were significantly higher than those found for both the epileptic conditions in all regions excluding the right frontal region. EC<sub>NS</sub> showed lower IAF values in comparison to EC<sub>WS</sub> in almost all cortical regions.

### 3.1.1. Statistical comparisons of EEG cortical sources

To further investigate the impact of BECTS on the cortical sources of resting state EEG rhythms, we computed TSMs in the five frequency bands under the EC<sub>NS</sub> and EC<sub>WS</sub> conditions (Figs 5–7, S2–4). Fig. S5 shows the spatial extent of the distributed sources of interictal spikes localized using eLORETA and averaged across all patients. As shown, only the right centro-temporal regions are highly involved in the generation of the spikes.

Compared to controls, patients exhibited increased  $\theta$ ,  $\alpha$  and  $\beta_2$  activity under both conditions in the right centrotemporal regions, which are involved in the generation and propagation of the spikes. However, the spectral power increases of cortical sources were more pronounced in the presence of CTS, and were also observed in  $\beta_1$  in the right centrotemporal region and its immediately surrounding regions.

In patients, the right temporo-parieto-occipital junction also showed increased  $\theta$  and  $\alpha$  activities under the EC<sub>NS</sub> condition (Fig. 5). However,

the presence of CTS within EEG segments increased power in higher frequencies ( $\beta_1$  and  $\beta_2$ ) in the right temporo-parieto-occipital junction (Fig. S4). Furthermore, in patients, the bilateral temporal poles displayed increased cortical activities in all five-frequency bands under both conditions. To a lesser degree, the left centrotemporal area including the insula also exhibited increased power in all bands.

Compared to controls, patients were characterized by significantly decreased power in all bands in bilateral frontal and occipital lobes, especially in the presence of CTS. Other spurious increases/decreases in the power of various bands were also observed in deeper structures (see supplementary figures).

## 4. Discussion

This study was the first attempt to investigate differences in the topographic distribution of EEG relative and absolute spectral power and EEG cortical sources between healthy control subjects and patients with BECTS under the eyes-closed resting state condition in five frequency bands. Our findings demonstrated that BECTS has a profound effect on the spectral power of resting state EEG activities and cortical sources by activating/deactivating cortical regions.

In the sensor space, we found significant increases in relative and absolute  $\theta$  power in all brain regions especially in the epileptogenic zone in the right centrotemporal region in comparison to healthy controls. Meanwhile, the  $\theta$  power decreased in frontal and occipital regions in comparison to central region of epileptic patients. This observation is consistent with results from other studies conducted on Temporal Lobe Epileptic patients (TLE) (Quraan et al., 2013). Several studies (Clemens, 2004; Clemens et al., 2000; Douw et al., 2010; Schneebaum-Sender et al., 2012) have reported enhanced  $\theta$  power in children with epilepsy with and without medication in comparison to controls (Clemens et al., 2010). However, it has been shown that the increased theta power in some cerebral regions is more pronounced in epileptic patients taking anti-epileptic drugs (Béla et al., 2007; Clemens, 2008; Clemens et al., 2006; Kikumoto et al., 2006). Nevertheless, in our study the drug effect can be ruled out to explain the spectral differences between the EC<sub>NS</sub> (eyes-closed without spike) and EC<sub>WS</sub> (eyes-closed with spike) conditions.

Significant increases in  $\theta$ ,  $\alpha$ , and  $\beta$  cortical sources were observed in the source space of the right centrotemporal area, the region of CTS generation, under the EC<sub>WS</sub> condition. Centrotemporal spikes are known to be highly reproducible sharp waves with similar morphological characteristics, high amplitudes and durations of more than 70 ms corresponding to frequencies above the  $\theta$  band (Panayiotopoulos, 1999a,b). Therefore, in our analysis, the increased relative power in frequencies

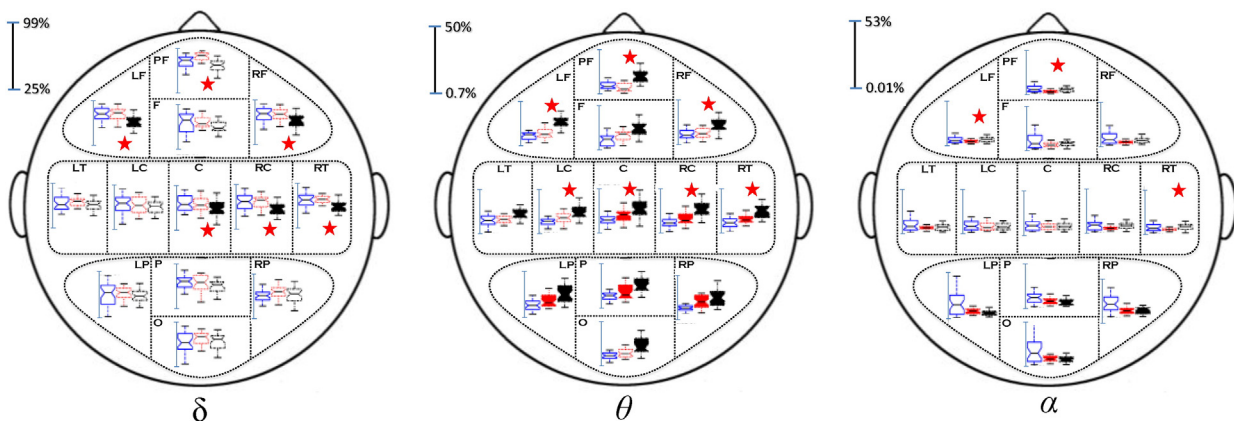


**Fig. 3.** Average normalized spectral power maps ( $\pm$  standard deviation) in the sensor space under the eyes-closed condition for the control group (EC<sub>CT</sub>, left boxplots), patient group (EC<sub>NS</sub>, no spike condition, middle boxplots) and patient group (EC<sub>WS</sub>, with spike condition, right boxplots) in  $\delta$ ,  $\theta$  and  $\alpha$  bands. Significant differences between EC<sub>CT</sub> and EC<sub>NS</sub>/EC<sub>WS</sub> are shown in solid boxplots. Asterisks indicate statistically significant differences ( $p < 0.01$ ) between EC<sub>NS</sub> and EC<sub>WS</sub>.

**Table 3**  
Absolute power ( $\mu V^2/Hz$ ) computed for each region, frequency band and all the conditions.

Region	Freq. Band	$\delta$ mean $\pm$ std	$\theta$ mean $\pm$ std	$\alpha$ mean $\pm$ std	$\beta_1$ mean $\pm$ std	$\beta_2$ mean $\pm$ std
PF	EC <sub>CT</sub>	0.0504 $\pm$ 0.0013	0.0076 $\pm$ 0.0003	0.0049 $\pm$ 0.0008	0.0013 $\pm$ 0.0001	0.0005 $\pm$ 0.0000
	EC <sub>WS</sub>	0.0444 $\pm$ 0.0009	0.0135 $\pm$ 0.0018	0.0035 $\pm$ 0.0002	0.0001 $\pm$ 0.0000	0.0003 $\pm$ 0.0001
	EC <sub>NS</sub>	0.0604 $\pm$ 0.0007	0.0073 $\pm$ 0.0007	0.0018 $\pm$ 0.0025	0.0008 $\pm$ 0.0009	0.0004 $\pm$ 0.0035
L	EC <sub>CT</sub>	0.0495 $\pm$ 0.0014	0.0072 $\pm$ 0.0003	0.0052 $\pm$ 0.0009	0.0016 $\pm$ 0.0001	0.0008 $\pm$ 0.0001
	EC <sub>WS</sub>	0.04010 $\pm$ 0.005	0.0146 $\pm$ 0.0011	0.0040 $\pm$ 0.0004	0.0012 $\pm$ 0.0002	0.0004 $\pm$ 0.0003
	EC <sub>NS</sub>	0.0535 $\pm$ 0.0074	0.0082 $\pm$ 0.0068	0.0026 $\pm$ 0.0028	0.0012 $\pm$ 0.0009	0.0007 $\pm$ 0.0005
F	EC <sub>CT</sub>	0.0465 $\pm$ 0.0022	0.0089 $\pm$ 0.0006	0.0068 $\pm$ 0.0011	0.0019 $\pm$ 0.0002	0.0007 $\pm$ 0.0001
	EC <sub>WS</sub>	0.0481 $\pm$ 0.0048	0.0167 $\pm$ 0.0009	0.0056 $\pm$ 0.0009	0.0022 $\pm$ 0.0002	0.0007 $\pm$ 0.0002
	EC <sub>NS</sub>	0.0483 $\pm$ 0.0032	0.0130 $\pm$ 0.0010	0.0049 $\pm$ 0.003	0.0027 $\pm$ 0.0001	0.0012 $\pm$ 0.0009
RF	EC <sub>CT</sub>	0.0473 $\pm$ 0.0018	0.0074 $\pm$ 0.0004	0.0051 $\pm$ 0.0008	0.0016 $\pm$ 0.0001	0.0007 $\pm$ 0.0001
	EC <sub>WS</sub>	0.0425 $\pm$ 0.0041	0.0123 $\pm$ 0.0015	0.0044 $\pm$ 0.0004	0.0015 $\pm$ 0.0002	0.0006 $\pm$ 0.0001
	EC <sub>NS</sub>	0.0557 $\pm$ 0.0021	0.0083 $\pm$ 0.0077	0.0029 $\pm$ 0.0034	0.0015 $\pm$ 0.0013	0.0007 $\pm$ 0.0001
LC	EC <sub>CT</sub>	0.0390 $\pm$ 0.0017	0.0088 $\pm$ 0.0006	0.0088 $\pm$ 0.0007	0.0019 $\pm$ 0.0002	0.0007 $\pm$ 0.0001
	EC <sub>WS</sub>	0.0369 $\pm$ 0.0051	0.0128 $\pm$ 0.0012	0.0044 $\pm$ 0.0007	0.0015 $\pm$ 0.0003	0.0004 $\pm$ 0.0001
	EC <sub>NS</sub>	0.0403 $\pm$ 0.0062	0.0102 $\pm$ 0.0006	0.0048 $\pm$ 0.0042	0.0015 $\pm$ 0.0015	0.0005 $\pm$ 0.0002
C	EC <sub>CT</sub>	0.0411 $\pm$ 0.0020	0.0097 $\pm$ 0.0004	0.0080 $\pm$ 0.0010	0.0017 $\pm$ 0.0002	0.0005 $\pm$ 0.0001
	EC <sub>WS</sub>	0.0367 $\pm$ 0.0041	0.0157 $\pm$ 0.0011	0.0047 $\pm$ 0.0008	0.0012 $\pm$ 0.0002	0.0003 $\pm$ 0.0001
	EC <sub>NS</sub>	0.0382 $\pm$ 0.0021	0.0118 $\pm$ 0.0074	0.0039 $\pm$ 0.0030	0.0011 $\pm$ 0.00105	0.0003 $\pm$ 0.0002
RC	EC <sub>NS</sub>	0.0422 $\pm$ 0.0017	0.0076 $\pm$ 0.0004	0.0081 $\pm$ 0.0007	0.0017 $\pm$ 0.0002	0.0007 $\pm$ 0.0001
	EC <sub>WS</sub>	0.0381 $\pm$ 0.0046	0.0157 $\pm$ 0.0014	0.0055 $\pm$ 0.0011	0.0015 $\pm$ 0.0002	0.0003 $\pm$ 0.0001
	EC <sub>NS</sub>	0.0420 $\pm$ 0.0037	0.0103 $\pm$ 0.0063	0.0035 $\pm$ 0.0031	0.0014 $\pm$ 0.0012	0.0005 $\pm$ 0.0004
LT	EC <sub>CT</sub>	0.0460 $\pm$ 0.0009	0.0094 $\pm$ 0.0006	0.0079 $\pm$ 0.0007	0.0018 $\pm$ 0.0001	0.0007 $\pm$ 0.0001
	EC <sub>WS</sub>	0.0405 $\pm$ 0.0033	0.0126 $\pm$ 0.0020	0.0041 $\pm$ 0.0005	0.0016 $\pm$ 0.0002	0.0007 $\pm$ 0.0001
	EC <sub>NS</sub>	0.0432 $\pm$ 0.0052	0.0111 $\pm$ 0.0051	0.0036 $\pm$ 0.0037	0.0018 $\pm$ 0.0017	0.0009 $\pm$ 0.0010
RT	EC <sub>CT</sub>	0.0456 $\pm$ 0.0016	0.0085 $\pm$ 0.0004	0.0063 $\pm$ 0.0006	0.0020 $\pm$ 0.0002	0.0007 $\pm$ 0.0001
	EC <sub>WS</sub>	0.0429 $\pm$ 0.0029	0.0149 $\pm$ 0.0014	0.0054 $\pm$ 0.0004	0.0016 $\pm$ 0.0001	0.0005 $\pm$ 0.0001
	EC <sub>NS</sub>	0.0467 $\pm$ 0.0032	0.0104 $\pm$ 0.0082	0.0031 $\pm$ 0.0038	0.0015 $\pm$ 0.0011	0.0007 $\pm$ 0.0000
LP	EC <sub>CT</sub>	0.0434 $\pm$ 0.0021	0.0101 $\pm$ 0.0005	0.0197 $\pm$ 0.0014	0.0023 $\pm$ 0.0003	0.0005 $\pm$ 0.0000
	EC <sub>WS</sub>	0.0385 $\pm$ 0.0043	0.0155 $\pm$ 0.0016	0.0053 $\pm$ 0.0010	0.0013 $\pm$ 0.0003	0.0003 $\pm$ 0.0001
	EC <sub>NS</sub>	0.0422 $\pm$ 0.0056	0.0116 $\pm$ 0.0087	0.0048 $\pm$ 0.0064	0.0013 $\pm$ 0.0013	0.0003 $\pm$ 0.0008
P	EC <sub>CT</sub>	0.0370 $\pm$ 0.0020	0.0079 $\pm$ 0.0006	0.0109 $\pm$ 0.0014	0.0016 $\pm$ 0.0002	0.0004 $\pm$ 0.0001
	EC <sub>WS</sub>	0.0346 $\pm$ 0.0023	0.0149 $\pm$ 0.0023	0.0041 $\pm$ 0.0008	0.0011 $\pm$ 0.0002	0.0003 $\pm$ 0.0000
	EC <sub>NS</sub>	0.0401 $\pm$ 0.0034	0.0129 $\pm$ 0.0093	0.0041 $\pm$ 0.0036	0.0011 $\pm$ 0.0012	0.0002 $\pm$ 0.0013
RP	EC <sub>CT</sub>	0.0394 $\pm$ 0.0015	0.0089 $\pm$ 0.0004	0.00173 $\pm$ 0.0017	0.0024 $\pm$ 0.0017	0.0003 $\pm$ 0.0003
	EC <sub>WS</sub>	0.0428 $\pm$ 0.0051	0.0153 $\pm$ 0.0002	0.00059 $\pm$ 0.0008	0.0014 $\pm$ 0.0002	0.0003 $\pm$ 0.0000
	EC <sub>NS</sub>	0.0443 $\pm$ 0.0076	0.0125 $\pm$ 0.0028	0.00043 $\pm$ 0.0044	0.0011 $\pm$ 0.0012	0.0003 $\pm$ 0.0001
O	EC <sub>CT</sub>	0.0426 $\pm$ 0.0018	0.0092 $\pm$ 0.0007	0.0173 $\pm$ 0.0004	0.0024 $\pm$ 0.0005	0.0006 $\pm$ 0.0000
	EC <sub>WS</sub>	0.0435 $\pm$ 0.0045	0.0136 $\pm$ 0.0024	0.0064 $\pm$ 0.0008	0.0013 $\pm$ 0.0002	0.0003 $\pm$ 0.0000
	EC <sub>NS</sub>	0.0482 $\pm$ 0.0056	0.0108 $\pm$ 0.0020	0.0051 $\pm$ 0.0008	0.0011 $\pm$ 0.0002	0.0002 $\pm$ 0.0000

above the  $\theta$  band can be simply explained by the presence of CTS in EEG segments.

The increase in relative power of higher frequencies especially several hundred milliseconds around CTS (Bourel-Ponchel, 2013; Gotman et al., 2005) resulted in a less significant increase in the power of low frequencies ( $\delta$  band). Under both conditions, in most frequency bands, similar trends of spectral changes were observed in BECTS patients, which may reflect the modulatory effect of epileptic networks on the

spectral power of cortical sources regardless of the presence of CTS in the scalp EEG segments analyzed. These findings indicate that, even in the absence of CTS in the scalp EEG, the activity of epileptic networks in BECTS has a profound impact on the EEG resting activity. This finding is consistent with those reported in other resting state studies (Ciumas et al., 2014; Kim et al., 2014; Pardoe et al., 2013). However, the presence of CTS clarified spectral differences between patients and controls with a wider spatial impact within the  $\beta_1$  band.

IAF differences between the groups may reflect decreased cognitive performances in patients as suggested in several studies (Angelakis et al., 2004; Khader et al., 2010; Klimesch et al., 1993). The lower IAF was correlated with lower power at parietal and occipital region especially under the EC<sub>WS</sub> condition. This finding might explain cognitive and attention impairment in BECTS patients (Holmes and Lenck-Santini, 2006; Metz-Lutz et al., 1999).

Another major finding of this study was the increased relative  $\theta$  and  $\alpha$  power under the EC<sub>NS</sub> condition, and the increased relative  $\alpha$ ,  $\beta_1$  and  $\beta_2$  power under the EC<sub>WS</sub> condition consistently in the right temporo-parieto-occipital (TPO) junction. This finding may suggest that the epileptic zone in BECTS impairs the right temporo-parieto-occipital region. The temporo-parieto-occipital region is believed to be involved in high level neurological functions (De Benedictis et al., 2014), especially auditory, visual, somatosensory and memory processes. Impairment of the TPO in children with epilepsy has been shown to be associated with higher activity in this region (Barba et al., 2007; Besseling et al., 2013; Hewett et al., 2011; Tang et al., 2014), which is likely to have neurobiological relevance determined by anatomical development and neurocognitive factors (Jiang et al., 2015; Tang et al., 2014). The

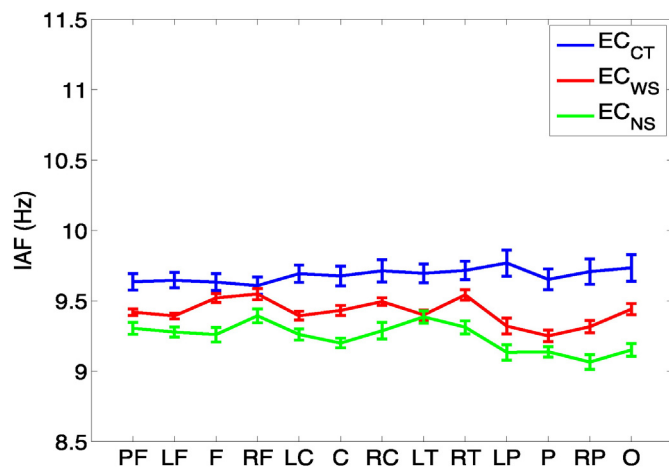


**Fig. 4.** Individual alpha frequency (IAF) for all the 13 regions (see Fig. 2 for abbreviations).

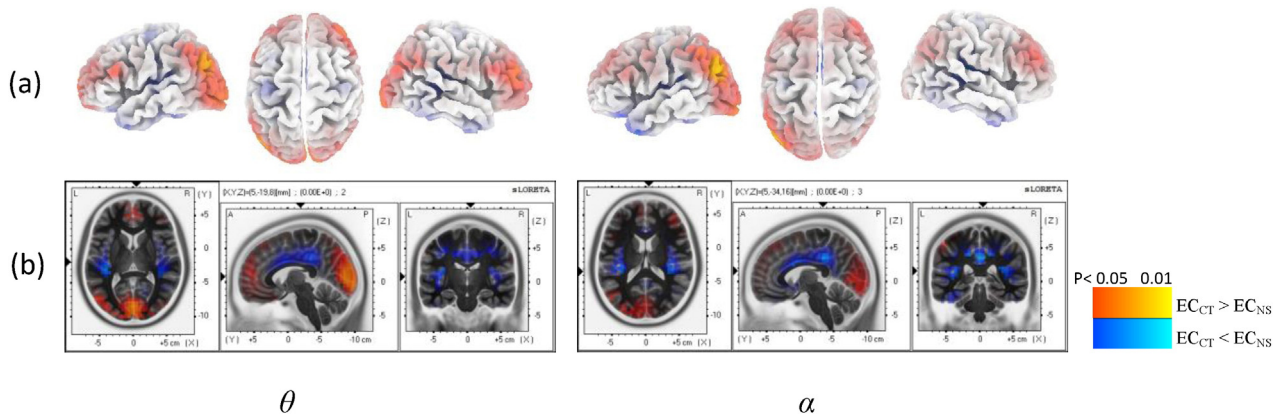


**Fig. 5.** Statistical maps of differences between cortical sources computed under the eyes-closed condition for the control group ( $EC_{CT}$ , left boxplots) and the patient group ( $EC_{NS}$ , no spike condition, right boxplots) in  $\theta$  and  $\alpha$  bands. The results have been projected onto the cortical layer of the realistic head model (a) and the MNI152 MRI (b). Color bars indicate significant differences between  $EC_{CT}$  and  $EC_{NS}$ , red ( $EC_{CT} > EC_{NS}$ ) and blue ( $EC_{CT} < EC_{NS}$ ).

disconnection or resection of TPO in children with epilepsy has been shown to increase the likelihood of alternative epilepsy treatment (Ansari et al., 2010; Mohamed et al., 2011), which may indicate the involvement of the TPO region in epileptic networks.

The bilateral increases in all bands under both conditions in the poles of the temporal lobes, known to be the regions responsible for language and speech processing, suggest possible interhemispheric synchronization in temporal regions due to CTS. Several studies (Ay et al., 2009; Baglietto et al., 2001; Kossoff et al., 2007; Liasis et al., 2006; Metz-Lutz et al., 1999; Northcott et al., 2007) have discussed the impaired visual and auditory networks and alternation of source activities at the bilateral poles of the temporal lobes in BECTS patients.

A compelling finding of the present study was the decreased activities of cortical sources in the frontal and occipital lobes in BECTS patients compared to healthy subjects in all frequency bands and conditions, notably under the  $EC_{WS}$  condition. The frontal and occipital cortical depression in BECTS patients is likely to be associated with decreased activity of the default mode network (Archer et al., 2003; Blumenfeld et al., 2004; Fahoum et al., 2013; Gotman et al., 2005; Ibrahim et al., 2014; Laufs et al., 2007; Ligot et al., 2014; Yang et al., 2014). This finding is also in line with the frontal decrease in the relative power of lower frequencies observed in the time-frequency domain several hundred milliseconds before and after centrotemporal spikes in BECTS patients (Bourel-Ponchel, 2013). The reduced activity of the prefrontal and frontal lobes might also explain some of the cognitive impairments and other brain malfunctions related to benign epilepsy (Holmes and Lenck-Santini, 2006; Weglage et al., 1997), as it has been shown that any

dysfunction in this region in childhood is likely to affect cognitive development (Badre et al., 2009; Stuss and Alexander, 2000).

Certain discrepancies between the topographic distribution of scalp EEG relative spectral power (in the sensor space) and the spatial distribution of cortical sources (in the source space) in different frequency bands were observed in this study. In our study, the increased or decreased cortical activities in various frequency bands estimated by means of the eLORETA approach were not expected to exactly follow the same spatial pattern of the spectral changes obtained using power spectrum analysis in the sensor space. The discrepancies can be explained by methodological differences between the approaches. Our STP maps were obtained by averaging the relative power values over groups of electrodes in each of 13 regions, while eLORETA maps were t-maps generated from statistical analysis of all 6234 voxels, whose source activities were estimated using all electrodes. *Frequency-domain eLORETA* generally provides better results for EEG resting analysis because the estimated neuronal generator distribution, when using this approach, does not depend on the polarity of the scalp EEG maps (Pascual-Marqui, 2014).

A potential limitation of our study is the sample size. For the thirteen cerebral regions, we computed the minimum sample size (Freedman et al., 2001) with the statistical power of 80%. The average sample size required for performing statistical comparisons between the groups was about 7 which was less than the sample sizes (eleven patients and twelve controls) set in our study.

Our overall findings indicate that, in addition to the dysfunction of the right centrotemporal region, which is the epileptic focus, cortical depression of frontal and occipital regions may show resting network

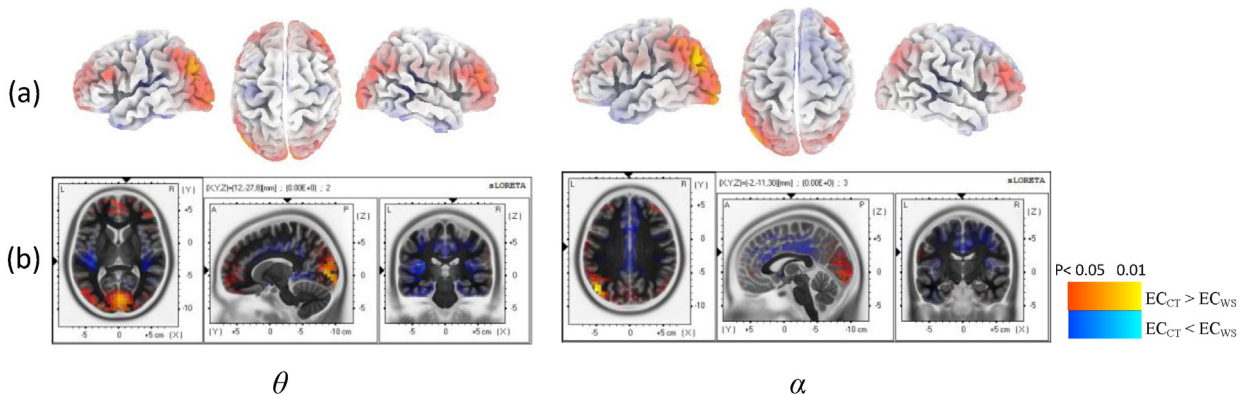


**Fig. 6.** Statistical maps of differences between cortical sources computed under the eyes-closed condition for the control group ( $EC_{CT}$ , left boxplots) and patient group ( $EC_{WS}$ , with spike condition, right boxplots) in  $\theta$  and  $\alpha$  bands. The results have been projected onto the cortical layer of the realistic head model (a) and the MNI152 MRI (b). Color bars indicate significant differences between  $EC_{CT}$  and  $EC_{WS}$ , red ( $EC_{CT} > EC_{WS}$ ) and blue ( $EC_{CT} < EC_{WS}$ ).

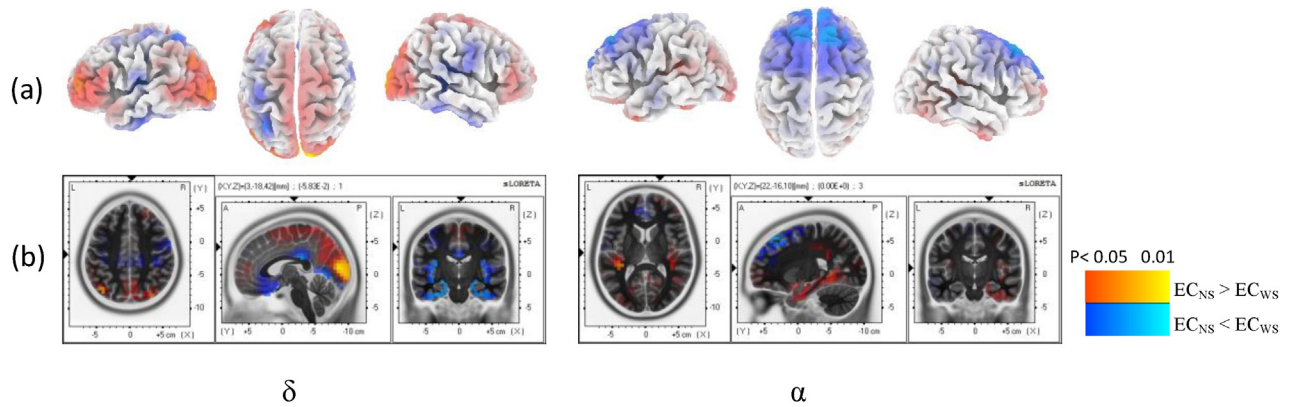


**Fig. 7.** Statistical maps of differences between cortical sources computed under the no-spike ( $EC_{NS}$ , left boxplots) and with-spike ( $EC_{WS}$ , right boxplots) eyes-closed conditions in  $\delta$  and  $\alpha$  bands for the epileptic group. The results have been projected onto the cortical layer of the realistic head model (a) and the MNI152 MRI (b). Color bars indicate significant differences between  $EC_{NS}$  and  $EC_{WS}$ , red ( $EC_{NS} > EC_{WS}$ ) and blue ( $EC_{NS} < EC_{WS}$ ).

disruption in benign childhood epilepsy with centrotemporal spikes. These findings encourage further investigation into the impact of BECTS on the resting state networks.

## Appendix A. Supplementary data

Supplementary data associated with this article can be found online at <http://dx.doi.org/10.1016/j.nicl.2015.08.014>.

## References

- Angelakis, E., Lubar, J.F., Stathopoulou, S., Kounios, J., 2004. Peak alpha frequency: an electroencephalographic measure of cognitive preparedness. *Clin. Neurophysiol. Off. J. Int. Fed. Clin. Neurophysiol.* 115 (4), 887–897. <http://dx.doi.org/10.1016/j.clinph.2003.11.03415003770>.
- Ansari, S.F., Maher, C.O., Tubbs, R.S., Terry, C.L., Cohen-Gadol, A.A., 2010. Surgery for extratemporal nonlesional epilepsy in children: a meta-analysis. *Childs Nerv. Syst. ChNS Off. J. Int. Soc. Pediatr. Neurosurg.* 26 (7), 945–951. <http://dx.doi.org/10.1007/s00381-009-1056-720013124>.
- Archer, J.S., Abbott, D.F., Waites, A.B., Jackson, G.D., 2003. fMRI “deactivation” of the posterior cingulate during generalized spike and wave. *NeuroImage* 20 (4), 1915–1922. [http://dx.doi.org/10.1016/S1053-8119\(03\)00294-514683697](http://dx.doi.org/10.1016/S1053-8119(03)00294-514683697).
- Ay, Y., Gokben, S., Serdaroglu, G., Polat, M., Tosun, A., Tekgul, H., Solak, U., Kesikci, H., 2009. Neuropsychologic impairment in children with rolandic epilepsy. *Pediatr. Neurol.* 41 (5), 359–363. <http://dx.doi.org/10.1016/j.pediatrneurol.2009.05.01319818938>.
- Babiloni, C., Pistoia, F., Sarà, M., Vecchio, F., Buffo, P., Conson, M., Onorati, P., Albertini, G., Rossini, P.M., 2010. Resting state eyes-closed cortical rhythms in patients with locked-in-syndrome: an EEG Study. *Clin. Neurophysiol. Off. J. Int. Fed. Clin. Neurophysiol.* 121 (11), 1816–1824. <http://dx.doi.org/10.1016/j.clinph.2010.04.02720541461>.
- Badre, D., Hoffman, J., Cooney, J.W., D’Esposito, M., 2009. Hierarchical cognitive control deficits following damage to the human frontal lobe. *Nat. Neurosci.* 12 (4), 515–522. <http://dx.doi.org/10.1038/nm.227719252496>.
- Baglietto, M.G., Battaglia, F.M., Nobili, L., Tortorelli, S., De Negri, E., Calevo, M.G., Veneselli, E., De Negri, M., 2001. Neuropsychological disorders related to interictal epileptic discharges during sleep in benign epilepsy of childhood with centrotemporal or rolandic spikes. *Dev. Med. Child Neurol.* 43 (6), 407–412. <http://dx.doi.org/10.1017/S00126220100075511409830>.
- Barba, C., Barbatì, G., Minotti, L., Hoffmann, D., Kahane, P., 2007. Ictal clinical and scalp-EEG findings differentiating temporal lobe epilepsies from temporal “plus” epilepsies. *Brain J. Neurol.* 130 (7), 1957–1967. <http://dx.doi.org/10.1093/brain/awm10817535836>.
- Béla, C., Mónika, B., Márton, T., István, K., 2007. Valproate selectively reduces EEG activity in anterior parts of the cortex in patients with idiopathic generalized epilepsy. A low resolution electromagnetic tomography (LORETA) study. *Epilepsy Res.* 75 (2–3), 186–191. <http://dx.doi.org/10.1016/j.eplepsyres.2007.06.00917624734>.
- Besseling, R.M.H., Jansen, J.F.A., Overvliet, G.M., van der Kruijs, S.J.M., Vles, J.S.H., Ebus, S.C.M., Hofman, P.A.M., de Louw, A., Aldenkamp, A.P., Backes, W.H., 2013. Reduced functional integration of the sensorimotor and language network in rolandic epilepsy. *NeuroImage Clin.* 2, 239–246. <http://dx.doi.org/10.1016/j.nicl.2013.01.00424179777>.
- Blom, S., Brorson, L.O., 1966. Central spikes or Sharp waves (Rolandic spikes) in children’s EEG and their clinical significance. *Acta Paediatr Scand* 55 (4), 385–393. <http://dx.doi.org/10.1111/j.1651-2227.1966.tb08809.x5966338>.
- Blumenfeld, H., McNally, K.A., Vanderhill, S.D., Paige, A.L., Chung, R., Davis, K., Norden, A.D., Stokking, R., Studholme, C., Novotny, E.J., Zupal, I.G., Spencer, S.S., 2004. Positive and negative network correlations in temporal lobe epilepsy. *Cereb. Cortex* 14 (8), 892–902. <http://dx.doi.org/10.1093/cercor/bhh04815084494>.
- Bocquillon, P., Dujardin, K., Betrouni, N., Phalempin, V., Houdayer, E., Bourriez, J.-L., Derambure, P., Szurhaj, W., 2009. Attention impairment in temporal lobe epilepsy: a neurophysiological approach via analysis of the P300 wave. *Hum. Brain Mapp.* 30 (7), 2267–2277. <http://dx.doi.org/10.1002/hbm.2066619034898>.
- Bourel-Ponchel, E., 2013. Exploration de l’unité neurovasculaire dans l’épilepsie de l’enfant: approche multimodale haute densité couplant l’EEG à l’imagerie optique fonctionnelle. Amiens.
- Camfield, C.S., Berg, A., Stephani, U., Wirrell, E.C., 2014. Transition issues for benign epilepsy with centrotemporal spikes, nonlesional focal epilepsy in otherwise normal children, childhood absence epilepsy, and juvenile myoclonic epilepsy. *Epilepsia* 55 (Suppl. 3), 16–20. <http://dx.doi.org/10.1111/epi.1270625209080>.
- Cataldi, M., Avoli, M., de Villers-Sidani, E., 2013. Resting state networks in temporal lobe epilepsy. *Epilepsia* 54 (12), 2048–2059. <http://dx.doi.org/10.1111/epi.1240024117098>.
- Ciomas, C., Saignavongs, M., Iliski, F., Herbillon, V., Laurent, A., Lothe, A., Heckemann, R.A., de Bellescize, J., Panagiotakaki, E., Hannoun, S., Marinier, D.S., Montavont, A., Ostrowsky-Coste, K., Bedoin, N., Ryvlin, P., 2014. White matter development in children with benign childhood epilepsy with centro-temporal spikes. *Brain J. Neurol.* 137 (4), 1095–1106. <http://dx.doi.org/10.1093/brain/awu03924598359>.
- Clemens, B., 2004. Pathological theta oscillations in idiopathic generalised epilepsy. *Clin. Neurophysiol.* 115 (6), 1436–1441. <http://dx.doi.org/10.1016/j.clinph.2004.01.01815134712>.
- Clemens, B., 2008. Valproate decreases EEG synchronization in a use-dependent manner in idiopathic generalized epilepsy. *Seizure* 17 (3), 224–233. <http://dx.doi.org/10.1016/j.seizure.2007.07.00517697790>.
- Clemens, B., Bessenyei, M., Fekete, I., Puskás, S., Kondákor, I., Tóth, M., Hollódy, K., 2010. Theta EEG source localization using LORETA in partial epilepsy patients with and without medication. *Clin. Neurophysiol. Off. J. Int. Fed. Clin. Neurophysiol.* 121 (6), 848–858. <http://dx.doi.org/10.1016/j.clinph.2010.01.02020181513>.
- Clemens, B., Majoros, E., 1987. Sleep studies in benign epilepsy of childhood with rolandic spikes. II. Analysis of discharge frequency and its relation to sleep dynamics. *Epilepsia* 28 (1), 24–27.
- Clemens, B., Ménes, A., Piros, P., Bessenyei, M., Altmann, A., Jerney, J., Kollár, K., Rosdy, B., Rózsavölgyi, M., Steinecker, K., Hollódy, K., 2006. Quantitative EEG effects of carbamazepine, oxcarbazepine, valproate, lamotrigine, and possible clinical relevance of the findings. *Epilepsy Res.* 70 (2–3), 190–199. <http://dx.doi.org/10.1016/j.eplepsyres.2006.05.00316765028>.
- Clemens, B., Sziget, G., Barta, Z., 2000. EEG frequency profiles of idiopathic generalised epilepsy syndromes. *Epilepsy Res.* 42 (2–3), 105–115. [http://dx.doi.org/10.1016/S0920-1211\(00\)00167-411074183](http://dx.doi.org/10.1016/S0920-1211(00)00167-411074183).
- De Benedictis, A., Duffau, H., Paradiso, B., Grandi, E., Balbi, S., Granieri, E., Colarusso, E., Chioffi, F., Marras, C.E., Sarubbo, S., 2014. Anatomico-functional study of the temporo-parieto-occipital region: dissection, tractographic and brain mapping evidence from a neurosurgical perspective. *J. Anat.* 225 (2), 132–151. <http://dx.doi.org/10.1111/joa.1220424975421>.
- Douw, L., van Dellen, E., de Groot, M., Heimans, J.J., Klein, M., Stam, C.J., Reijnen, J.C., 2010. Epilepsy is related to theta band brain connectivity and network topology in brain tumor patients. *B.M.C. Neurosci.* 11, 103. <http://dx.doi.org/10.1186/1471-2202-11-10320731854>.
- Fahoum, F., Zelmann, R., Tyvaert, L., Dubeau, F., Gotman, J., 2013. Epileptic discharges affect the default mode network – fMRI and intracerebral EEG evidence. *PLOS One* 8 (6), e68038. <http://dx.doi.org/10.1371/journal.pone.0068038>.
- Freedman, K.B., Back, S., Bernstein, J., 2001. Sample size and statistical power of randomised, controlled trials in orthopaedics. *J. Bone Joint Surg. Br.* 83 (3), 397–402. <http://dx.doi.org/10.1302/0301-620X.83B3.1058211341427>.
- Gotman, J., Grova, C., Bagshaw, A., Kobayashi, E., Aghakhani, Y., Dubeau, F., 2005. Generalized epileptic discharges show thalamocortical activation and suspension of the default state of the brain. *Proc. Natl. Acad. Sci. U. S. A.* 102 (42), 15236–15240. <http://dx.doi.org/10.1073/pnas.050493510216217042>.
- Grech, R., Cassar, T., Muscat, J., Camilleri, K.P., Fabri, S.G., Zervakis, M., Xanthopoulos, P., Sakkalis, V., Vanrumste, B., 2008. Review on solving the inverse problem in EEG source analysis. *J. Neuroengineering Rehabil.* 5, 25. <http://dx.doi.org/10.1186/1743-0003-5-2518990257>.

